

Article

Analysis of a Wind-Driven Air Compression System Utilising Underwater Compressed Air Energy Storage

Lawrie Swinfen-Styles , Seamus D. Garvey, Donald Giddings, Bruno Cárdenas  and James P. Rouse

Department of Mechanical, Materials and Manufacturing Engineering, University of Nottingham, Nottingham NG7 2RD, UK; seamus.garvey@nottingham.ac.uk (S.D.G.); donald.giddings@nottingham.ac.uk (D.G.); bruno.cardenas@nottingham.ac.uk (B.C.); james.rouse@nottingham.ac.uk (J.P.R.)

* Correspondence: lawrie.swinfen-styles@nottingham.ac.uk

Abstract: The increasing push for renewable penetration into electricity grids will inevitably lead to an increased requirement for grid-scale energy storage at multiple time scales. It will, necessarily, lead to a higher proportion of the total energy consumed having been passed through storage. Offshore wind is a key technology for renewable penetration, and the co-location of energy storage with this wind power provides significant benefits. A novel generation-integrated energy storage system is described here in the form of a wind-driven air compressor feeding underwater compressed air energy storage. A direct drive compressor would require very high intake swept volumes. To overcome this difficulty, some prior compression is introduced. This paper discusses the constituent technologies for this concept, as well as the various configurations that it might take and the logic behind operating it. Special consideration has been given to the differences resulting from utilising a near-isothermal wind-driven compressor versus a near-adiabatic one. Multiple iterations of the system have been simulated. This has been done using a price-matching algorithm to optimise the system operation and using volumetric air flow rates to calculate exergy flow. Simulated operation has been performed for a year of real wind and electricity price data. This work has been performed in order to clarify the relationships between several key parameters in the system, including pressure and work ratios, volumetric flowrates, storage costs and profit rates. An additional objective of this paper was to determine whether the system has the potential for economic viability in some future energy grid, especially when compared with alternative wind and energy storage solutions. The results of the simulation indicated that, with proper sizing, the system might perform competitively with these alternatives. Maximum one-year return on investment values of 9.8% for the isothermal case and 13% for the adiabatic case were found. These maxima were reached with ~15–20 h of output storage. In all cases, it was found that maximising the power of the wind-driven compressor compared with the initial compressor was favourable.

Keywords: generation integrated energy storage; wind-integrated energy storage; compressed air energy storage; underwater compressed air energy storage; wind-driven air compression; intake swept volumes; capture value; alternative wind technology; wind system simulation; optimal operation of energy stores



Citation: Swinfen-Styles, L.; Garvey, S.D.; Giddings, D.; Cárdenas, B.; Rouse, J.P. Analysis of a Wind-Driven Air Compression System Utilising Underwater Compressed Air Energy Storage. *Energies* **2022**, *15*, 2142. <https://doi.org/10.3390/en15062142>

Academic Editors: Alon Kuperman and Alessandro Lampasi

Received: 12 January 2022

Accepted: 7 March 2022

Published: 15 March 2022

Publisher's Note: MDPI stays neutral with regard to jurisdictional claims in published maps and institutional affiliations.



Copyright: © 2022 by the authors. Licensee MDPI, Basel, Switzerland. This article is an open access article distributed under the terms and conditions of the Creative Commons Attribution (CC BY) license (<https://creativecommons.org/licenses/by/4.0/>).

1. Introduction

Large-scale energy storage will likely play a significant role in any future energy system that wishes to implement high levels of renewable penetration [1]. This is due to its ability to provide much-needed flexibility in grids whose generation portfolio will become increasingly inflexible as a result of the natural variability of renewable sources. This widely accepted notion has led to a surge in the number and scope of energy storage technologies, both proposed and implemented.

Most of the work done in the energy storage sector has focused on standalone storage systems, which absorb electricity and convert to and from some other storable form of

energy before re-supplying (a proportion of) the electricity at a later time. Standalone storage can be developed and implemented entirely separately from the generation, enabling traditional renewable energy technologies to be used for generation. There are also non-grid applications for energy storage, such as the use of Li-ion batteries in electric vehicles, that are, by definition, standalone.

In contrast to standalone storage, generation-integrated energy storage (GIES) technologies store energy before it is converted to electricity [2]. Figure 1 contrasts the energy conversions seen in GIES systems with those in standalone storage.

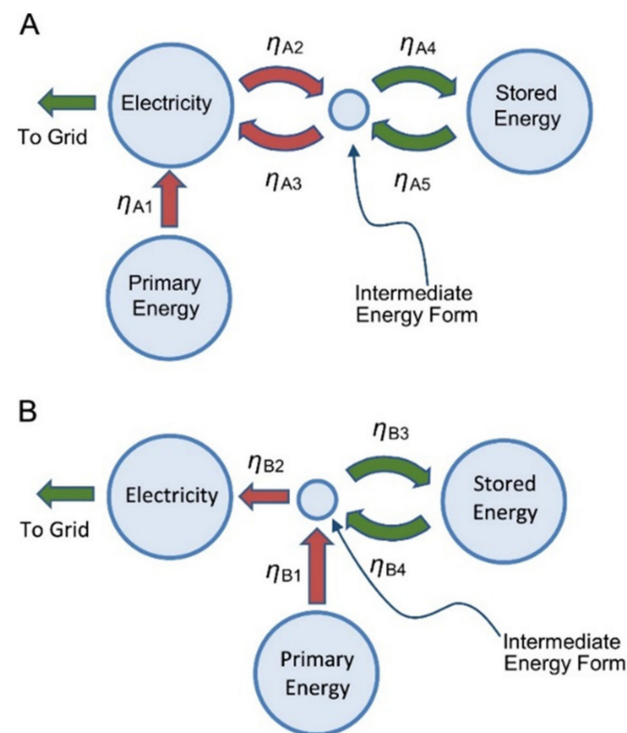


Figure 1. Comparison of energy conversions between (A) standalone and (B) generation-integrated energy storage configurations. From [2].

GIES systems minimise the conversions between the primary energy collected and the consumed output electricity for any energy that passes through storage. A familiar example of a GIES system is natural hydro, where the energy from flowing water is converted into a storable form (gravitational potential via damming) before it is ever passed through turbines to generate electricity. Although pure transmission efficiencies (that is, the output exergy divided by the input exergy for exergy that does not pass through storage) may be slightly lower than in conventional generation systems, GIES systems have the potential to achieve significantly higher efficiencies for energy that has passed through storage. Such GIES systems may therefore achieve higher overall throughput efficiencies than systems with independent generation and storage, if a sufficient proportion of the total output energy is required to pass through storage, as represented in Figure 2 (from [2]). GIES systems therefore have the potential to be relatively cheap forms of energy storage. Additional examples of well-established GIES technologies include many concentrated solar plants [3,4]. GIES systems have also been proposed for wind [5–8] and nuclear power [9,10].

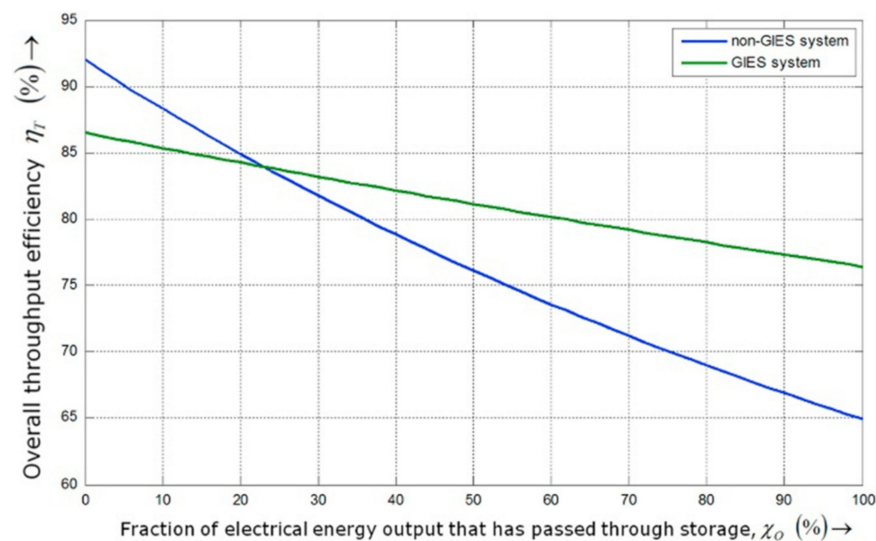


Figure 2. Overall throughput efficiency against fraction of output energy that passed through storage for standalone and GIES stores. From [2].

An offshore wind-driven GIES system that exercises multiple stages of air compression, with integrated compressed air energy storage, is proposed in [11]. This paper clarifies and expands upon that idea. In Section 2, the technologies that constitute the system are explained and examples of other systems utilising them are given. In Section 3, the system from [11] is described, with particular note to possible alternative configurations. Section 4 describes simulations of the system that were performed in order to understand the relationships between parameters such as storage size and pressure ratio. The economic benefits of such a system are then discussed, along with the barriers impeding it.

2. Constituent Technologies

2.1. Isothermal and Adiabatic Compressed Air Energy Storage

Compressed air energy storage (CAES) is a set of thermomechanical energy storage technologies. In CAES, work is done on ambient air in order to compress it to a higher pressure, at which point it is stored (at near-ambient temperature) for some period of time before being expanded back to ambient conditions to generate electricity. Two grid-scale CAES plants in Huntorf, Germany, and Alabama, USA, are diabatic (D-CAES), meaning that the heat from compression is discarded and the air is stored cool, before being reheated prior to expansion. In these cases, the pre-heating of air is done through the burning of natural gas. For several reasons, not least of which is the desire not to use fossil fuels in energy storage, modern CAES proposals tend towards Isothermal (I-CAES) or Adiabatic (A-CAES) configurations, which do not consume any combustible fuel, although CAES systems that use some carbon-neutral fuel (such as green hydrogen) have also been posited [12–14].

In I-CAES systems, air is compressed and expanded near-isothermally with the use of effective heat transfer. In a successful implementation, almost no exergy is lost, because any heat taken from the air is close to ambient temperature and therefore has negligible exergetic content. Assuming ideal gas behaviours, the work done on a volume of gas compressed isothermally is given by:

$$W_{ISO} = p_1 V_1 \ln\left(\frac{p_2}{p_1}\right) =: p_1 V_1 \ln(r), \quad (1)$$

where p is the gas pressure, V is the gas volume and subscripts 1 and 2 denote inlet and outlet, respectively.

Conversely, A-CAES systems purposely minimise the heat transfer between the air and its surroundings. In A-CAES, the heat is stripped from the air after compression and is then stored in thermal energy stores. For adiabatic compression, the work done on a gas is:

$$W_{ADIA} = p_1 V_1 \frac{\left(r^{((\gamma-1)/\gamma)} - 1 \right)}{((\gamma-1)/\gamma)} =: p_1 V_1 \frac{(r^\chi - 1)}{\chi}, \quad (2)$$

where $\gamma = 1.4$ for diatomic gases. As before, r represents the pressure ratio p_2/p_1 .

2.2. Wind-Driven Energy Storage

Integrating energy storage into wind power generation has been proposed in various formats. The simplest form of this is the co-location of a conventional energy store with wind turbines, used to smooth the intermittency of renewable generation [15–17]. If sufficiently inexpensive, this has some economic advantages for the operator, as electricity can be supplied to the grid during periods of higher value. There is also a benefit to the grid by reducing transmission losses. However, such systems cannot be described as GIES. Wind farms providing energy in the form of electricity to some co-located energy store could be described as “wind-powered”.

By contrast, “wind-driven” systems are defined here as those that initially convert the energy provided by the wind into a form of energy other than electricity. The majority of wind-driven GIES systems in the literature involve some form of gas compression, although the use of induction or other forms of direct heating have also been suggested [18].

Of the systems utilising gas compression, D-CAES [5], adiabatic compression [6] and offshore I-CAES [19] configurations have been proposed. In all cases, the gearbox of a conventional geared wind turbine—a source of considerable capital and maintenance cost—is removed, and the generator is relocated close to the energy stores at ground- or sea-level [20–22]. This leaves the nacelle of the wind turbine relatively free for compression machinery. In [19], a liquid piston compressor is used, with seawater performing the duty of the liquid and also acting as an excellent heat sink. Liquid piston technology is also used in [6], but is designed to perform near-adiabatically, with a radial piston configuration employing multiple stages to minimise the temperature gradients and therefore heat transfer.

2.3. Direct Drive Air Compression and the Problem of Intake Swept Volumes

The wind-driven CAES systems mentioned are direct drive, meaning that the compressor runs synchronous with the wind turbine itself. For most modern turbines, the tip-speed ratio (TSR) relates the tangential speed of the blade tips (u_{TIP}) to the oncoming wind speed (u):

$$TSR = \frac{u_{TIP}}{u} = \frac{\omega D}{2u}, \quad (3)$$

where ω is the rotational speed and D is the diameter of the turbine’s swept area. The rotational frequency of the rotor, f , is:

$$f = \frac{\omega}{2\pi} = \frac{uTSR}{\pi D}. \quad (4)$$

The parameters ω and f have rated values for any wind speed at or above the turbine’s rated wind speed u_R (and below its maximum wind speed). In this paper, the MHI Vestas V164-8.0 MW turbine will be used as the reference turbine. Data for this turbine is summarised in Table 1.

Table 1. Data for reference turbine used in this paper. From [23].

MHI Vestas V164-8.0 MW Turbine			
Name of Parameter	Parameter	Value	Units
Swept Diameter	D	164	m
Tip-speed	-	104	m/s
Rated windspeed	u_R	13	m/s
Cut-in speed	-	4	m/s
Cut-out speed	-	25	m/s
Tip-speed ratio	TSR	8	-
Rotational speed	ω	1.27	rad/s
Rotational frequency	f	0.20	rotations/s

For wind-driven compression, it is useful to find the intake swept volume of air, V_{swept} , that must be absorbed by the compressor in each rotation. This can be done by rearranging Equations (1) and (2), using the fact that the work done per rotation is equal to the rated power of the turbine $P_{turbine}$ divided by its rotational frequency. For isothermal compression, this gives:

$$V_{swept,ISO} = \frac{P_{turbine}}{f p_1 \ln(r)}, \quad (5)$$

and for adiabatic compression:

$$V_{swept,ADIA} = \frac{P_{turbine} \chi}{f p_1 (r^\chi - 1)}. \quad (6)$$

For a set upper pressure $p_2 = p_1 r$, a minimum swept volume is found in an isothermal compressor when $r = e \approx 2.7182$ and in an adiabatic compressor when $r = 1.4^{1/\chi} \approx 3.2467$. For pressure ratios above these optima, swept volumes increase much more slowly than for pressure ratios below these values (with V_{swept} tending to infinity as $r \rightarrow 1$).

For illustration, if air were to be compressed by the reference turbine from ambient pressure to 74 bar, the upper pressure of the D-CAES plant at Huntorf, an adiabatic compressor would need to intake 47.2 m³ of air per revolution and an isothermal compressor would need to intake 92.9 m³. It should be noted that the swept volume is relatively insensitive to the upper pressure. It has also been assumed here that the adiabatic compression would take place over a single stage (with regard to heat transfer). A multi-stage compressor might be used in a scenario where the upper temperature would be too high for conventional materials.

To estimate the acceptable swept volume for a compressor housed in a wind turbine, consider that the volume of both the gearbox and generator is freed up in a wind-driven system.

Assuming the use of a radial piston compressor design similar to that described in [6], the machine can be split into two distinct parts: here defined as the “displacer” and the “converter”. The displacer houses a camshaft and radial pistons and the converter contains the compression cylinders. It is therefore reasonable to make the approximation that the displacer replaces the gearbox and the converter replaces the generator in the turbine nacelle. The nacelle dimensions of the reference turbine are 24 × 12 × 7.5 m and the generator takes up approximately 1/8th of the total volume, or ~270 m³. A prototype compressor utilising the technology described in [6], in development at the University of Nottingham, has a ratio between the inlet swept volume and overall converter volume of roughly 0.004. Scaling up to the reference nacelle size, this relates to an intake swept volume of ~1.1 m³. Accounting for slightly larger allowable nacelles, as well as more optimised compressor geometries and nacelle layouts, it is likely that intake swept volumes of ~5–15 m³ might be achievable in the reference turbine. Even at the upper end of this

estimate, a turbine compressing to 74 bar would have a power of 2.54 MW (adiabatic) or 1.29 MW (isothermal)—only a fraction of the 8 MW reference turbine power.

The problem of large intake swept volumes is therefore significant for all direct drive systems. The I-CAES system in [19] solves this problem by moving the liquid piston to sea-level and instead utilising a variable displacement hydraulic pump in the nacelle. This combines well with the use of seawater as the liquid piston (thereby not requiring seawater to be pumped up to the nacelle). By contrast, Ref. [6] solves the problem of intake swept volumes by increasing the inlet air pressure p_1 . Rather than a CAES system, Ref. [6] is a pumped thermal energy storage system, wherein all exergy stored is in the form of high-grade heat (or coolth) that is stripped from the compressed gas [24]. This involves a closed gas loop, meaning that the inlet and outlet pressures for the compressor can be freely set.

2.4. Underwater Compressed Air Energy Storage

Underground caverns are often considered the default method of air storage when discussing CAES plants. The CAES plants in Huntorf and Alabama both use this method of storage, as do many other CAES proposals.

Such storage is generally isochoric (constant volume), meaning that emptying a proportion of the air in the store reduces the pressure of the remaining air. Expanders used in an isochoric CAES system must therefore run over a series of pressures, limiting their efficiency, as they cannot be optimised for a single pressure. As there will be a pressure below which an expander cannot run at an acceptable efficiency, this also significantly limits the proportion of the store that can be flexed. Cavern stability also limits operational pressure ranges, as a certain volume of “cushion gas” is required to ensure that the caverns do not collapse.

In contrast, isobaric (constant pressure) storage allows for the flexing of the entire storage volume, at a single pressure for which the expander can be optimised. Isobaric storage can be achieved in combined hydro-CAES plants where a water reservoir is used to keep constant pressure [25]. However, most isobaric storage designs revolve around the store being placed deep underwater, in a lake or ocean. This is known as underwater compressed air energy storage (UWCAES). In UWCAES, each 10 metres of water depth provides approximately 1 bar of additional pressure on the store. By filling the store with air of equivalent pressure to the hydrostatic pressure supplied by the water, the store itself does not need to provide any confining force. A UWCAES system utilising flexible canvas bags (energy bags) is described in [26,27] and expects storage capacity costs in the region of 25 \$/kWh (dependent on the storage depth). A representation of this design can be seen in Figure 3.

The components comprising an energy bag system are anchoring ballast (AB), tension cables (TC) and the canvas surface area itself (SU). The role of the tension cables is to counteract the buoyant force created by the air volume. The cables are therefore the sole structural element of the energy bag. It is explained in [26] that the cost of the anchoring ballast is proportional to the buoyancy force created by the energy bag volume and is therefore proportional to the cube of the characteristic dimension (the diameter, D) of the energy bag:

$$C_{AB} \propto D^3. \quad (7)$$

The tension cable cost is proportional to the product of its length L and tension force F_T , which is also proportional to the buoyancy force:

$$C_{TC} \propto LF_T \propto D^4. \quad (8)$$

The cost of the canvas is clearly proportional D^2 and so the total energy bag cost can be written as:

$$C_{BAG} = C_{AB} + C_{TC} + C_{SU} = aD^4 + bD^2 + cD^3, \quad (9)$$

where a , b and c are constants. By noting that the energy stored in the bag, E , is equal to another constant, k , multiplied by the energy bag volume,

$$\frac{C_{BAG}}{E} = \frac{aD^4 + bD^2 + cD^3}{kD^3}. \quad (10)$$

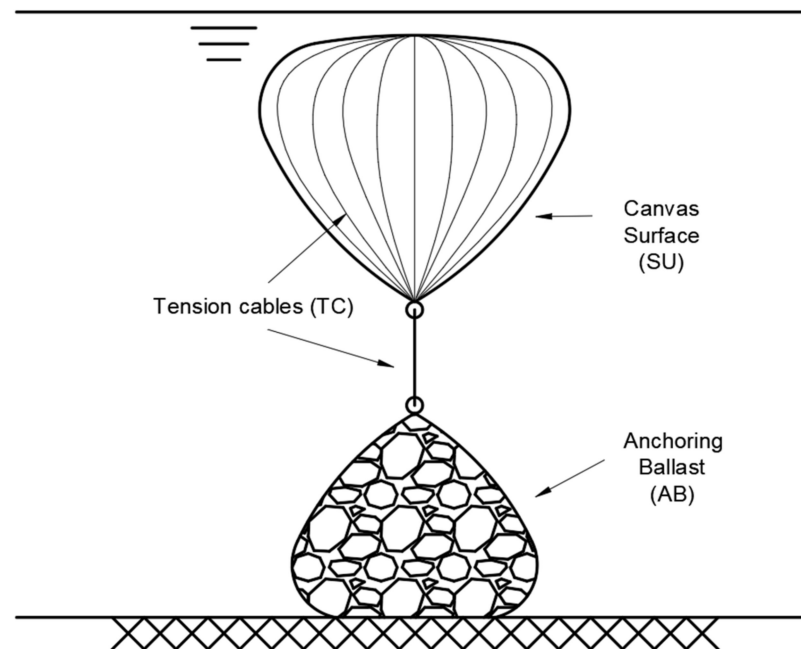


Figure 3. Energy bag underwater compressed air energy storage (UWCAES) system. Shown without pipework for simplicity.

Differentiating this to find the optimum and substituting into Equation (9) then shows that the optimum diameter is achieved when C_{SU} is equal to C_{TC} . Multiple energy bags of this optimal diameter would therefore be better value for money than a single energy bag of equivalent volume. The use of multiple smaller bags also has the benefit of reducing the proportion of storage that is out of service if damage to a single bag occurs. Assuming that any storage system employs multiple optimally sized energy bags (with the volumetric capacity of V_{opt}), the total cost of the system is the number of energy bags used multiplied by the cost of a single bag. Therefore, for a system with a volumetric capacity of nV_{opt} , where n is an integer, the total cost of the storage system is directly proportional to its volume.

The technologies discussed in this section have a clear synergy. The use of UWCAES specifically for the balancing of wind energy has been investigated previously [28,29]. However, iterations of this concept assume a conventional wind turbine with standalone UWCAES. Thus far, no literature has discussed the combination of wind-driven air compression with UWCAES. The possibility of utilising UWCAES in a GIES-type system is unexplored. The concept of wind-integrated energy storage itself (beyond the co-location of standalone energy storage) is underexplored.

Furthermore, no wind-driven air compression system attempts to solve the problem of large swept volumes with a prior stage of electrically driven air compression. It may initially seem counterintuitive to add electrically driven air compression to a wind-driven system. However, there is significant advantage to be had by removing the wind turbine gearbox and allowing direct drive air compression. There are also potential grid-balancing advantages to such a system, discussed later in this paper.

The system described in the remainder of this paper is not intended as a catch-all solution to the problem of inflexible wind generation. Indeed, it is a complimentary technology that might be used in tandem with a grid utilising any subset of systems

previously mentioned, conventional wind turbines, and large-scale standalone storage (for example, in the form of CAES or green hydrogen).

3. System Overview

3.1. Description

The system described in [11] is named *Wi-DACIS*, standing for wind-driven air compression and isobaric storage. It utilises the technologies previously mentioned in Section 2. A wind-driven, direct drive air compressor replaces the gearbox system in a conventional geared offshore wind turbine. The high-pressure air exhausted from the compressor can either be immediately expanded to generate electricity or passed into an energy bag air storage system. This provides flexibility to the otherwise intermittent renewable energy supply from the turbine. Because primary energy from the wind is used directly to compress air before it is ever converted into electricity, this constitutes a GIES system.

Being direct drive, the problem of intake swept volume must be considered. In a similar manner to the pumped heat system described in [6], the solution is to supply air to the primary compressor at a pressure higher than ambient. However, instead of the closed loop utilised by [6], *Wi-DACIS* employs a prior stage of compression, which absorbs air from the environment, compressing it from ambient conditions to a suitable pressure for the wind-driven compressor.

In [11], the *Wi-DACIS* system was originally described with two pressures of air store: a high-pressure store fed by the wind-driven compressor, and an additional medium-pressure store fed by the first stage compressor. While the authors believe that there could be significant merit to the additional flexibility provided by the medium-pressure store, the full cost/benefit analysis of such a store is beyond the scope of this paper and will be addressed in future work.

The classification of *Wi-DACIS* as a purely GIES system is dependent on the form that the first stage of compression takes. If it is driven by electricity from the grid, as is assumed for the analysis in Section 4, then it acts as a hybridisation of standalone and GIES systems, as some fraction of the energy in storage has been absorbed from the grid. The ratio of standalone to GIES utility is then dependent on the relative powers of the two compressor stages.

However, if the first stage of compression is run by some non-grid method (i.e., one in which electricity from the grid is not required, such as solar or wave power), then *Wi-DACIS* performs as a wholly GIES system. The possibility of using a form of trompe compressor as a method of offshore first-stage compression is also discussed in [11], using the water head created by wave heights to push volumes of water to a depth, pressurising the air entrained within that water.

Figure 4 shows the *Wi-DACIS* system in its hybrid GIES-standalone configuration, utilising a single high-pressure air store.

Important components and parameters for the *Wi-DACIS* system are:

- COMG—the grid-connected first stage of compression.
- COMW—the main stage, wind-driven compressor, which can be either isothermal or adiabatic (discussed in Section 3.2).
- HPEB—the high-pressure energy bag system (shown as a single bag for simplicity).
- EXP—the expander/generator set.
- HXU/TES—the heat-exchanger unit and thermal energy stores, relevant only if the main stage compressor is adiabatic.
- r_1 and r_2 —the pressure ratios of COMG and COMW. The pressure of the high-pressure store is $r_1 r_2$.
- P_G and P_W —the powers of COMG and COMW. P_{EXP} is the expander power.
- V_1, V_2, V_3 —the volumetric flowrate into COMG, out of COMG/into COMW and out of COMW/into EXP. p_1, p_2, p_3 are the respective pressures.

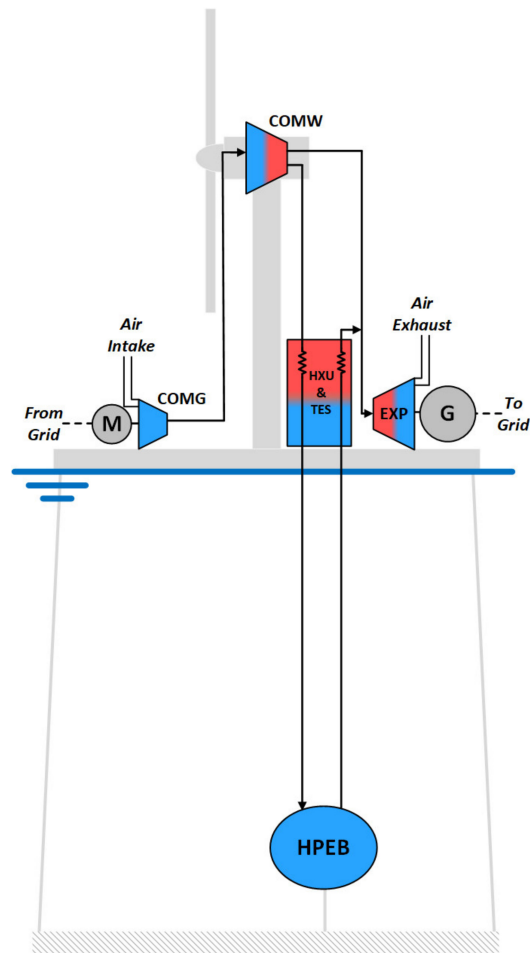


Figure 4. The *Wi-DACIS* system in an adiabatic main stage configuration. In an isothermal configuration, HXU and TES are not present.

3.2. Possible Configurations

An important consideration in a *Wi-DACIS* system is whether the main stage compressor is adiabatic or isothermal. This decision dictates several system parameters, including the relative powers (or relative pressure ratios, depending on which values are set) of the two compressors. Because the product of p and V remains constant throughout isothermal compression, if the main stage compressor is isothermal, the relative powers of the two stages can be described as:

$$\frac{P_G}{P_W} = \frac{\ln(r_1)}{\ln(r_2)}. \quad (11)$$

By comparison, if the main stage compressor is adiabatic, the relative powers can be described as:

$$\frac{P_G}{P_W} = \frac{\chi \ln(r_1)}{(r_2)^\chi - 1}. \quad (12)$$

Figure 5 shows that, for a set upper pressure $r_1 r_2$, an adiabatic main stage will result in a smaller grid-powered compressor. Given that the *Wi-DACIS* system intends the main-stage compressor to have a reasonably high power compared to the first-stage compressor (certainly $P_G/P_W < 1$), this limits the acceptable relative pressure ratios. In the example given in Figure 5, where $r_1 r_2 = 200$, r_2 would therefore need to be greater than 9 for an adiabatic main stage or greater than 14 for an isothermal one.

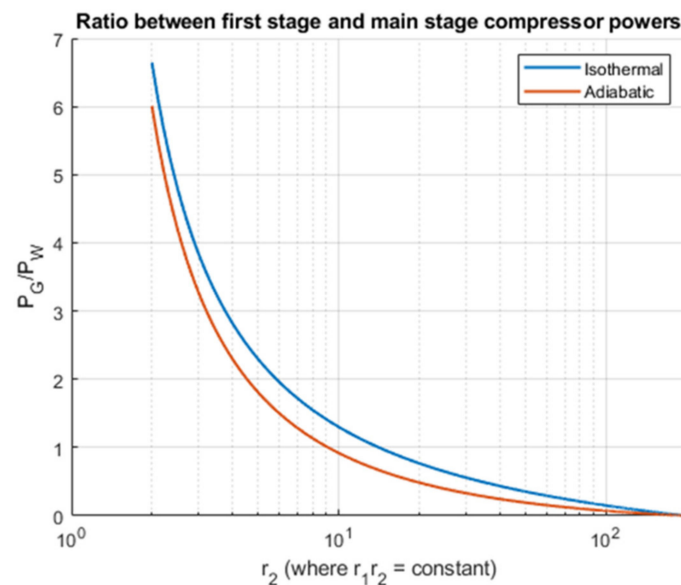


Figure 5. Power ratios for an isothermal and an adiabatic main stage of compression, where the upper pressure, $r_1 r_2$, is set.

The choice between isothermal and adiabatic compression also affects the required inlet swept volume, as is described in Section 2.3. For any given intake pressure and pressure ratio, an adiabatic compressor will require a lower intake swept volume than an isothermal one. This is due to the additional work done in adiabatic compression to heat the gas. As previously mentioned, the upper temperature is a limiting factor in the adiabatic case, but multi-stage compression is possible to keep this temperature within reasonable limits (by taking heat from the air at several points during the compression process).

With both of these effects taken into consideration, an adiabatic main stage appears to be the clear choice. However, this is also dependent on the relative costs of the compressors. Regardless of whether the main stage compressor is isothermal or adiabatic, heat exchange of some kind will be required, either in the form of inter-stage cooling, or to strip the heat from the air for storage. Assuming, then, that the isothermal and adiabatic compressors and heat exchangers are of similar costs, an important measure of the viability of adiabatic main stage compression is whether the thermal energy storage (TES) required by an adiabatic compressor is cost-competitive with the high-pressure energy bag system. Given that the costs calculations for the energy bags in Section 2.4 only include material costs, the same will be applied to the TES.

4. System Analysis

4.1. Simulation Data and Assumptions

Simulations of the *Wi-DACIS* system have been run for both the isothermal and adiabatic main-stage compressor configurations. These will provide insight into the relationship between various *Wi-DACIS* parameters, as well as providing a reasonable minimum size for the energy store and some sense of the profitability of such a system.

Wind speed data for 2015 were obtained from the UK Met Office Integrated Data Archive System (MIDAS) [30]. This took the form of sea-level wind speed data, which were converted to wind speed at turbine-height with:

$$u(z) = \frac{u_*}{\kappa} \left[\ln \left(\frac{z}{z_0} \right) \right], \quad (13)$$

where $u(z)$ is the wind speed at altitude z , u_* is the friction velocity, κ is the Von Kármán constant (~ 0.4) and z_0 is the roughness length (~ 0.0002 m for open sea) [31,32].

Hourly data from 12 locations were used (Figure 6). These sites were chosen due to the availability of sufficient wind speed data over the given period. Several of these sites would not necessarily be suitable for a *Wi-DACIS* system, due to their location on the continental shelf implying relatively shallow water. However, the data at these sites are sufficiently representative of generic offshore wind data to be suitable in the analysis. Figure 6 includes the approximate outline of the continental shelf, showing the closeness of the sites to relatively deep water. Figure 7 shows the worldwide water depth map. It is clear that a depth of 2000 m is closely accessible for much of the world's coastline.



Figure 6. Map of the 12 wind data point locations. Letters used to differentiate between sites. Adapted from [33] (Map Data: ©2022 Google, GeoBasis-DE/BKG ©2009).

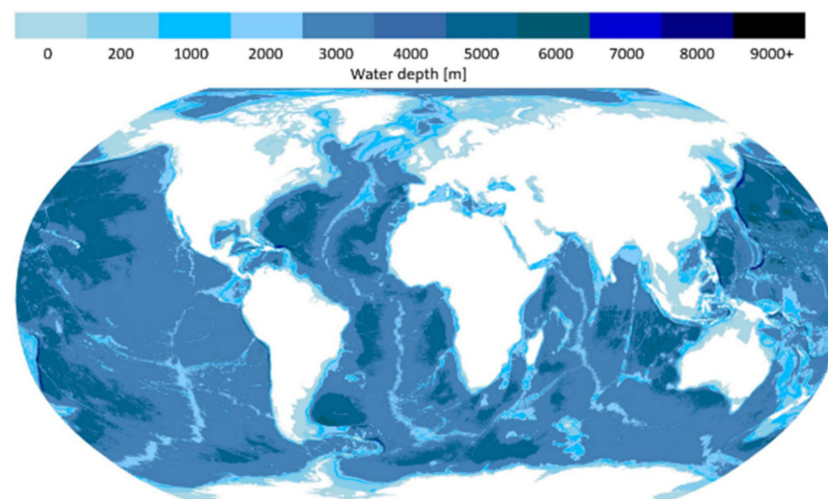


Figure 7. Map of worldwide water depth. Adapted from [34].

The wind speed data were converted to energy generation data using the real power curve of the reference turbine, shown in Figure 8 [23]. The energy generation data could then be used in the simulation to calculate the energy flow in the system via air volumetric flow rates.

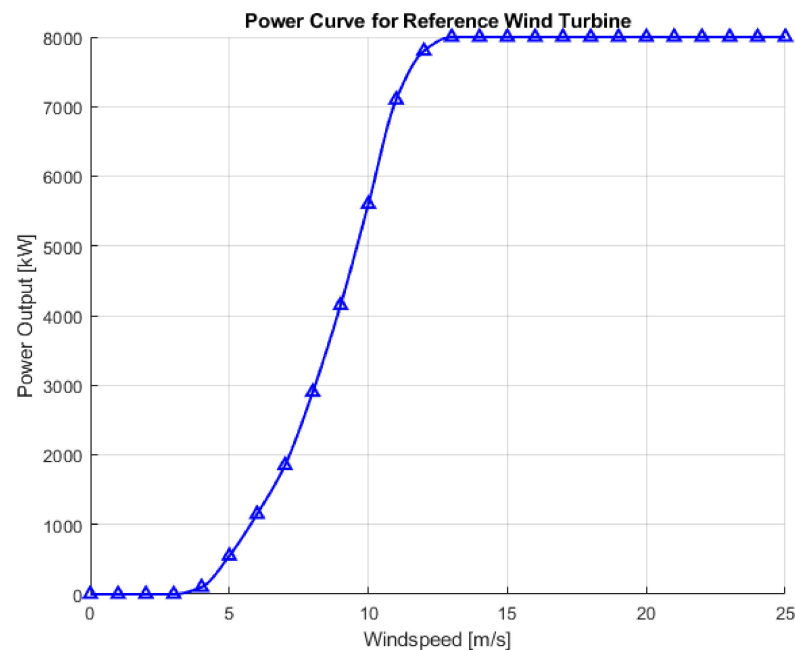


Figure 8. Power curve for reference wind turbine. Adapted from [23].

UK day-ahead electricity price data over the same 2015 time period were taken from [35]. It is assumed that the system operates with a merchant contract, using the hourly day-ahead electricity prices as a basis for decision-making. This is in contrast to many UK wind farms, which operate on the Contracts for Difference (CfD) scheme, wherein a single price is agreed upon per unit of electricity supplied to the grid, regardless of instantaneous electricity value. The revenue of a conventional wind turbine on the CfD scheme will also be considered for the sake of comparison.

The simulation assumes that the *Wi-DACIS* wind-driven compressor is capable of performing at part-load to the same extent as the conventional reference turbine. Optimal part-load performance would be made possible with a compressor design similar to the one described in [6], which allows individual compression cylinders to be deactivated via automated active valve control. It is expected that these operations could be performed at much shorter timescales than is required for the turbine blades to adjust pitch, meaning that overall part-load performance should not be affected.

The grid-powered isothermal compressor is assumed to be of sufficient power to provide the necessary volumetric flowrate to the main stage compressor at its nameplate capacity. It is also assumed to have no variation in efficiency at partial load.

In order to gain some measure of the cost of each iteration, unit costs were applied to each element of the system. Reasonable values for a , b and c from Equation (9) were found that satisfied the condition of a single optimum at $D \approx 20$ m and gave a cost of roughly 50 £/m^3 , indicated by [26]. The total energy bag storage was calculated as multiples of these optimal bags, with an additional smaller bag (if necessary) at a less optimal cost. It is assumed that each energy bag can store a parcel of air for as long as is required between the charging and discharging cycles. This is a reasonable assumption given the store sizes considered (<200 h).

4.2. Methodology

The initial inputs for the simulation can be split into system parameters and unit costs. The system parameters tested in the simulation are presented in Table 2.

Table 2. System parameters for *Wi-DACIS* simulations.

Name of Parameter	Parameter	Value(s)	Units
Main compressor swept volume	V_{swept}	~5–15	m ³ /rev
Maximum pressure	p_2	200	bar
High-pressure store size	-	1–200	hours

For each combination of store capacity and swept volume, the system powers, inlet and outlet volumetric flowrates, pressure ratios and energy bag sizes were calculated, both for the isothermal and adiabatic configurations. The initial state of charge (SoC) assumed for the store was 50% of the maximum charge. Operation over the year time period was then simulated for each system and at each site.

The simulation was performed assuming perfect knowledge of a year of day-ahead electricity prices and wind availability. A modified version of the price-matching algorithm found in [36] was used to find the optimal store and compressor power usage at each hour time interval.

The income (revenue) was calculated as a summation of the hour-wise multiplication of instantaneous electricity price and instantaneous expander power. Similarly, the expenditure was calculated as a summation of the hour-wise multiplication of instantaneous electricity price and the instantaneous power of the first-stage, grid-powered compressor.

For the configuration where the wind-driven stage is adiabatic, the required capacity of the thermal energy store was calculated using the work done by the adiabatic compressor from Equation (2), and the temperature was found by:

$$T_{store} = T_{ref} r_2^\chi, \quad (14)$$

where T_{ref} is the ambient temperature of the air. In a packed gravel bed TES, using a thermal medium (quartzite) with a specific heat capacity of 850 J/kg·K, the required mass was found:

$$m_{quartzite} = \frac{W_{Heat}}{850 \cdot (T_{store} - T_{ref})}. \quad (15)$$

The thermal medium was given a material cost of 0.1 GBP/kg [37]. A mass overrating factor of 2 was then applied.

An estimate of the steel required for the thermal store was obtained using a random sphere packing density ~0.64, quartzite and steel densities of 2700 kg/m³ and 8000 kg/m³, respectively, and assuming a TES store with a height to diameter aspect ratio of 2 and 20 mm thick walls (considered to be very conservative):

$$V_{store} = \frac{m_{quartzite}}{0.64 \times 2700}, \quad (16)$$

$$m_{steel} \approx 0.646(m_{quartzite})^{2/3}. \quad (17)$$

The cost of worked steel for wind turbines is in the order of 2 GBP/kg, based on assertions made by Henrik Stiesdal on several occasions, including at Floating Offshore Wind UK (30 October 2018) and the EWEA Floating Wind Power Debate (18 November 2015). Steel was therefore costed at 2 GBP/kg. The capital costs per unit power for the compressors and expanders were chosen partly from values in [2,13,38–40] and partly on the idea that a conventional wind turbine costs ~1 GBP/W and replacing the expensive gearbox element with an expensive compressor element will not change that value too significantly. These costs are summarised in Table 3. It should be noted that the cost (GBP/kW) for compressor and expander machinery is dependent on several factors, including its rated power—larger machines generally cost less per unit power [39–41]. In order to take advantage of the scalability in the *Wi-DACIS* system, it is likely that several turbines would be fed by a single

grid-powered compressor and would feed into a single expander. Although a single turbine has been simulated, this scalability has been accounted for in the capital costs chosen.

Table 3. Per-unit power capital costs for the compressor/expander machinery. Based on values in [2,13,38–40].

Machine	Cost Range (Nominal Value) (GBP/kW)
COMG	200–400 (300)
COMW	800–1200 (1000)
EXP	300–700 (500)

To reasonably account for losses in the system, the efficiencies shown in Table 4 were applied in the simulation. As with cost, the efficiency of machinery can be affected by its rated power [42,43]. The large scale of the machines used in *Wi-DACIS* means that the upper range of efficiencies is certainly accessible.

Table 4. Efficiencies of the system machinery used. Based on values in [44–48].

Machine	Efficiency Range, η (Nominal Value)
COMG	0.8–1.0 (0.9)
COMW	1 *
EXP	0.8–1.0 (0.9)
HPEB	0.98

* The efficiency value of the main stage compressor is given as 1 because it is a relative efficiency, which will be used to compare with alternative wind + storage systems in Section 4.5. The result of applying the COMG efficiency is that the pure transmission efficiency of the *Wi-DACIS* system will be 90% of the transmission efficiency of a conventional turbine.

The range of cost and efficiency values shown were used in data validation testing, whereas the nominal values were used in the main simulation.

The efficiency losses in the grid-powered compressor and the expander were accounted for by increasing the expenditure and decreasing the income by a factor of η , while keeping the actual exergy absorbed/sold the same.

Efficiency losses in the energy bags are expected to be extremely small. In this paper, a representative value of 0.98 was chosen. This was applied by increasing the cost of the stores by this factor.

The outputs of the simulations were: instantaneous compressor and expander powers over time, state of charge for the store over time, capital costs, revenue and expenditure (the difference of which is the profit), a one-year return on investment and potentially limiting parameters such as TES temperature and ratio of P_G/P_W .

4.3. Results and Discussion

Each of the 12 sites used in the simulation exhibited the same behaviours, although the exact values were slightly different due to local wind data. The averaged results of the 12 sites are used in the following figures. Maximum and minimum values given in the text cover all 12 sites.

The primary effect of increasing the inlet swept volume is that the main stage compressor, COMW, becomes a larger proportion of the total system power; alternatively, COMG becomes a smaller proportion. This is caused by the increased ratio r_2/r_1 , seen in Figure 9.

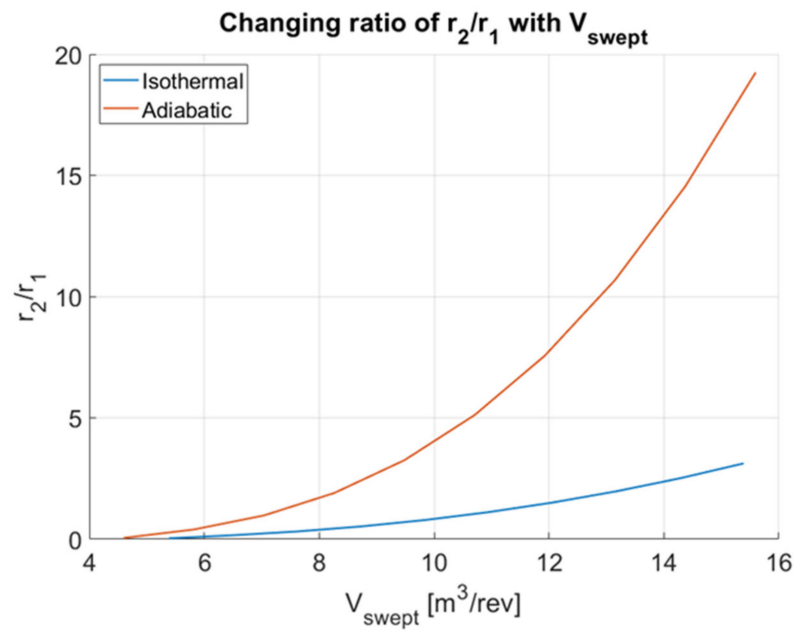


Figure 9. The relationship between the relative power of the main-stage and first-stage compressors and the intake swept volume, in the form of pressure ratio r_2/r_1 .

Increasing the proportional power of COMW in this way serves to significantly improve the yearly profit (income minus expenditure) of the system, in all iterations. This can be seen in Figure 10, which highlights the improvement of the system with increased V_{swept} (and reduced proportional power of COMG).

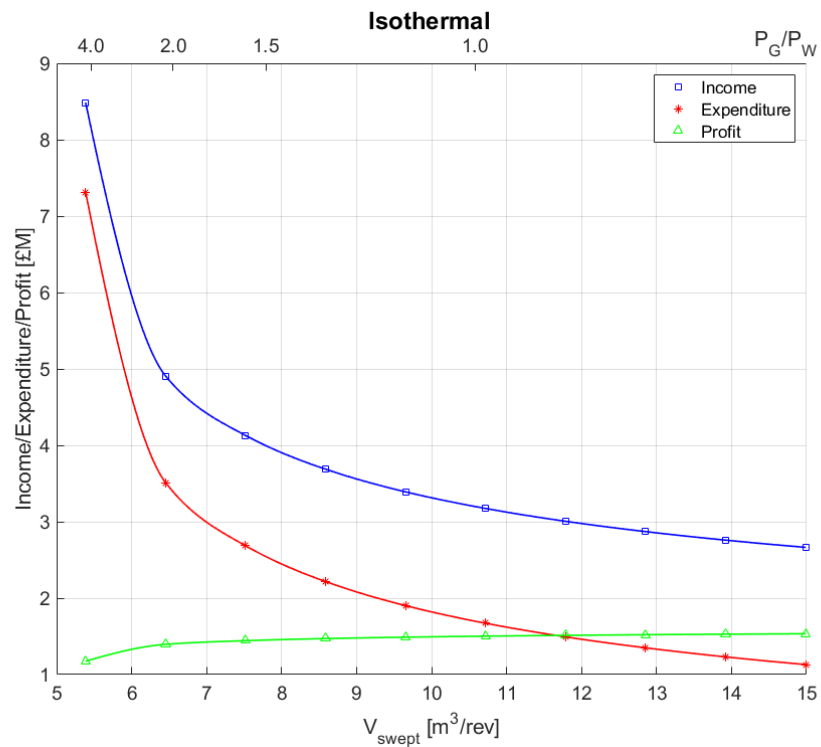


Figure 10. Cont.

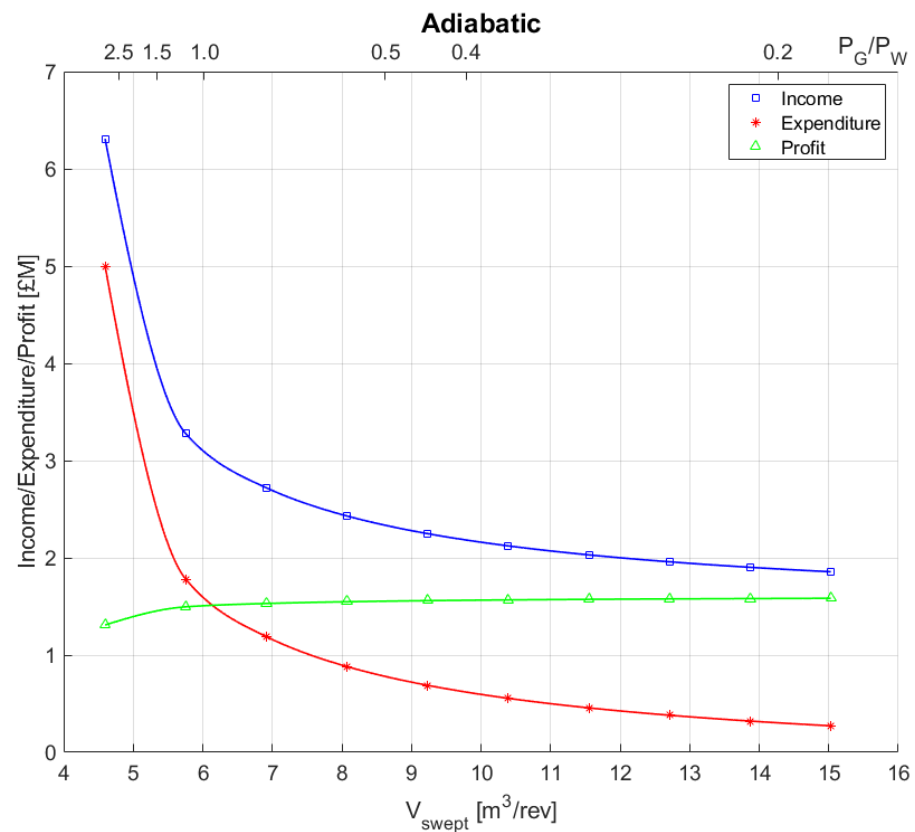


Figure 10. Income, expenditure and profit for representative isothermal (**above**) and adiabatic (**below**) systems with 200 h of storage. Also shown on the upper x-axes is the proportional power of COMG compared with COMW. Decreasing this ratio improves financial performance.

While the income of the system is reduced by increasing V_{swept} —a function of the total system power reducing as the proportional power of COMW, which is set at 8 MW, increases—the expenditure of the system decreases more quickly, resulting in greater profit. The expenditure is further reduced in the adiabatic case compared with the isothermal case, due to the further increase in the ratio between COMW and COMG powers, a result of the work of Equations (1) and (2).

Due to the effect the swept volume has on the system powers and pressure (and therefore costs), it is useful to show a breakdown of the cost elements with changing V_{swept} for both the isothermal and adiabatic cases. Figure 11 shows a breakdown of the cost elements for a system with 200 h of storage. Figure 12 normalises these costs by the power of the system at each value of V_{swept} .

For the adiabatic case, the reduction in the cost of the thermal energy store with increasing V_{swept} is due to the increasing pressure ratio of COMW. This results in a higher outlet air temperature; the thermal mass is therefore used more effectively. Likewise, the reduction in the cost of the air store is due to a larger proportion of the exergy being stored as heat, as V_{swept} increases.

Given that system capital costs are reduced and profits increased with increased V_{swept} , it is clear that the one-year return on investment (ROI) is significantly affected by increasing the inlet swept volume of the system. This can be seen in Figure 13, using a system with 200 h of storage for demonstration.

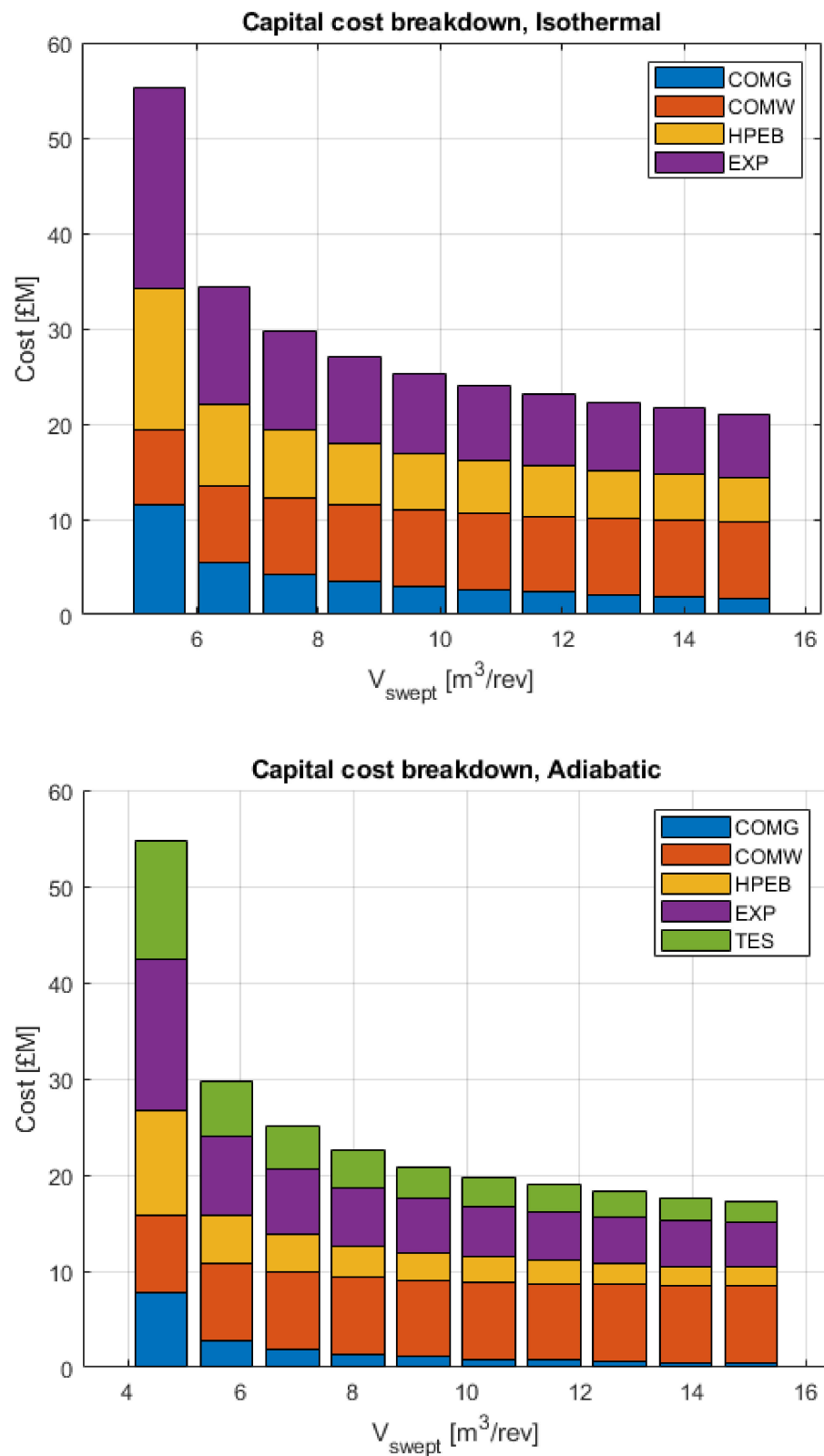


Figure 11. Breakdown of capital costs for an isothermal (**above**) and adiabatic (**below**) system with 200 h of storage.

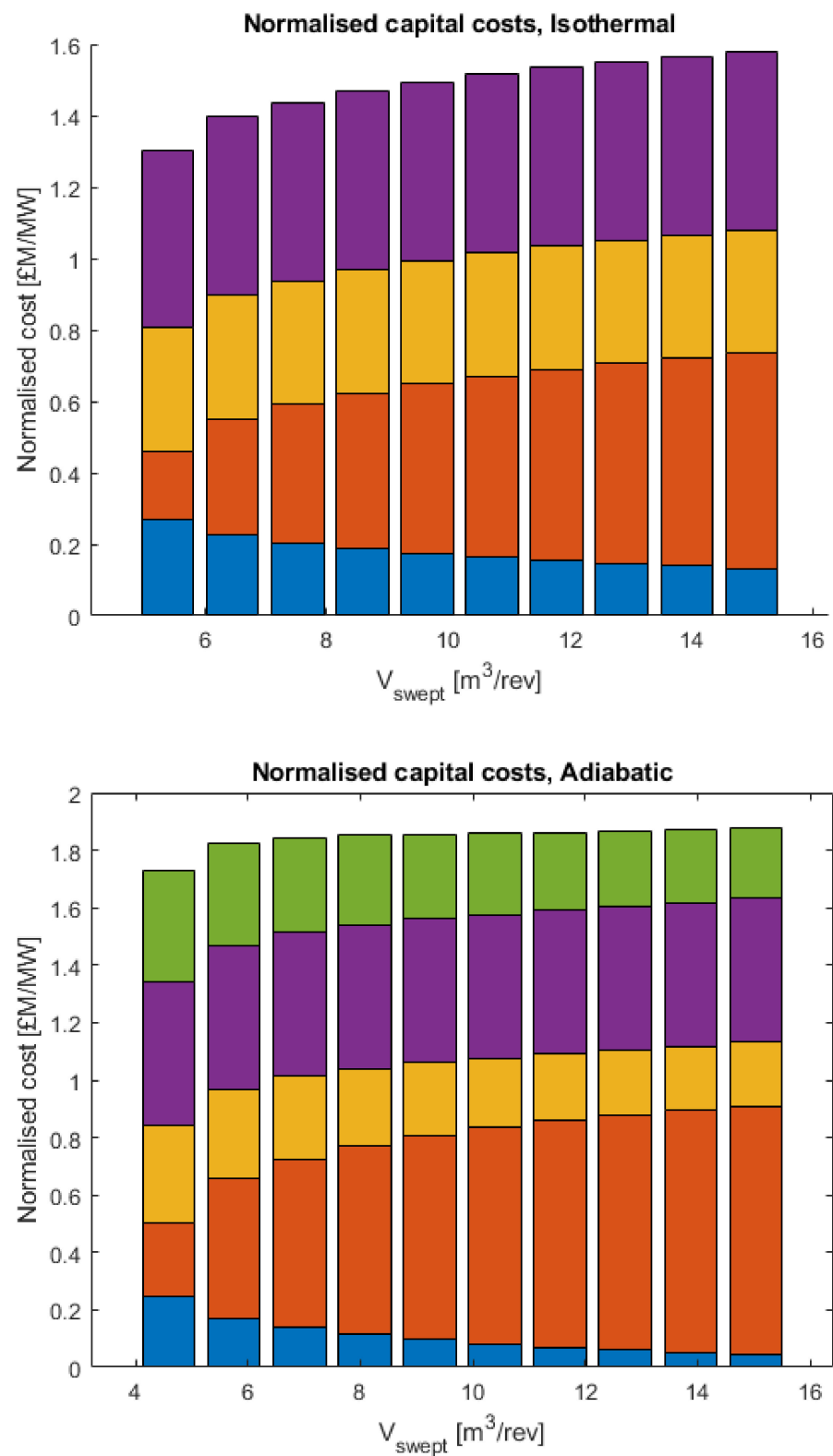


Figure 12. Breakdown of capital costs shown in Figure 10, normalised by the total discharge power of the system. Isothermal (above) and adiabatic (below) configurations shown.

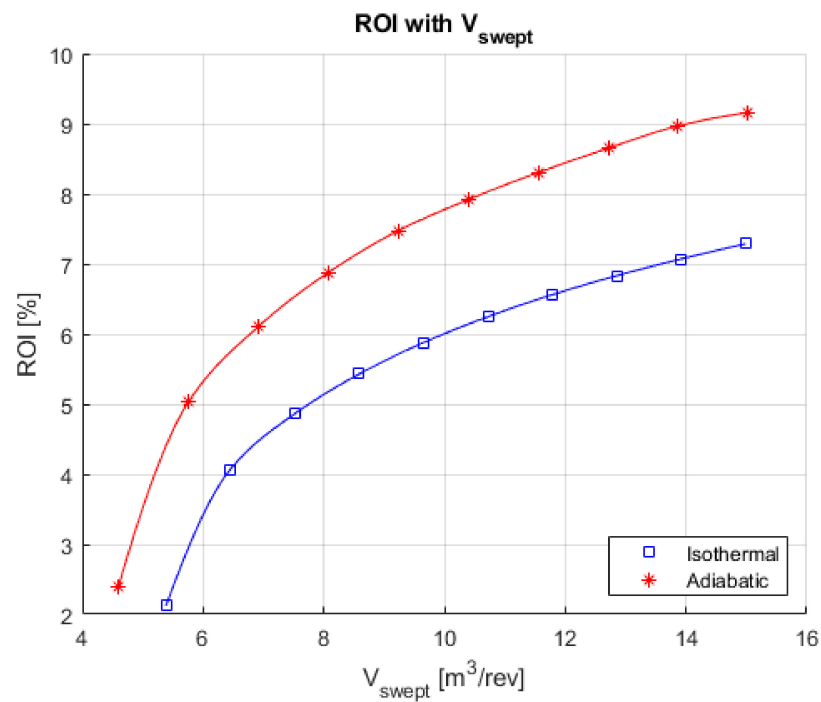


Figure 13. The relationship between one-year return on investment and inlet swept volume for a representative system with 200 h of storage.

It is therefore desirable for the profitability of the *Wi-DACIS* system to maximise V_{swept} to its upper practical limit.

It is important to determine whether there is an optimal energy storage capacity for the system. Figure 14 shows the ROI of a system with a constant swept volume and changing store size, from 1 to 200 h.

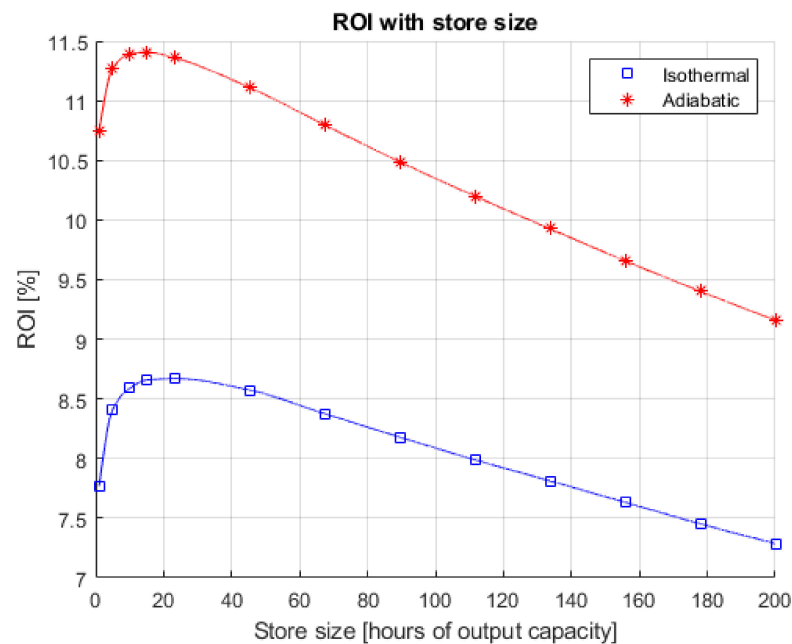


Figure 14. The relationship between one-year return on investment and storage capacity for a system with the maximum allowable inlet swept volume.

In fact, a maximum ROI for the system is reached in all cases. At the highest value of V_{swept} (shown in Figure 14), this occurs at ~20 h for the isothermal case and ~15 h for the adiabatic case. Before this point, there is very little value provided by the stores, despite the increased cost of the system compared with a conventional turbine (through the addition of the first-stage compressor and the expander). After this maximum, the increased value offered by the store does not make up for the climbing costs of such a system at present. This is summarised in Figures 15 and 16.

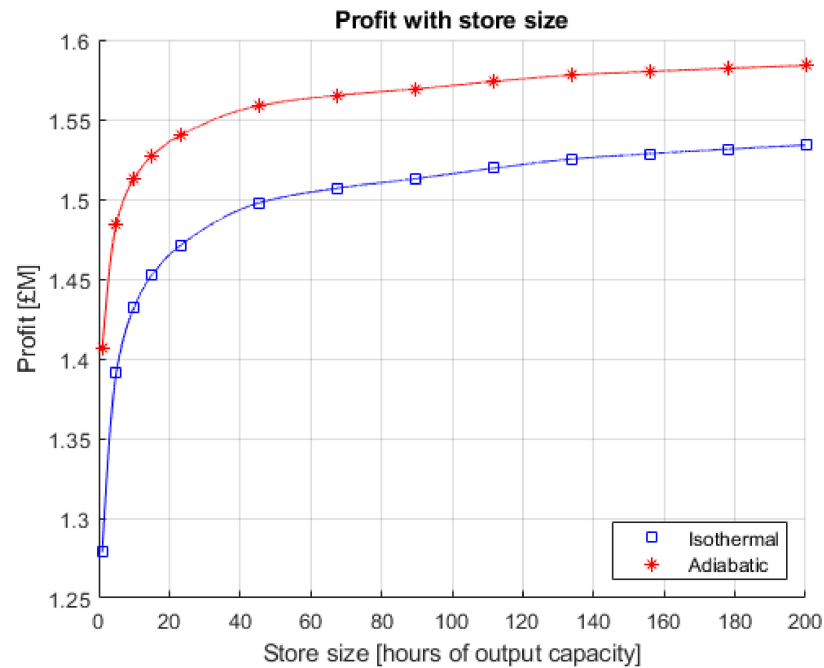


Figure 15. The relationship between profit and storage capacity for a representative system with the maximum allowable inlet swept volume.

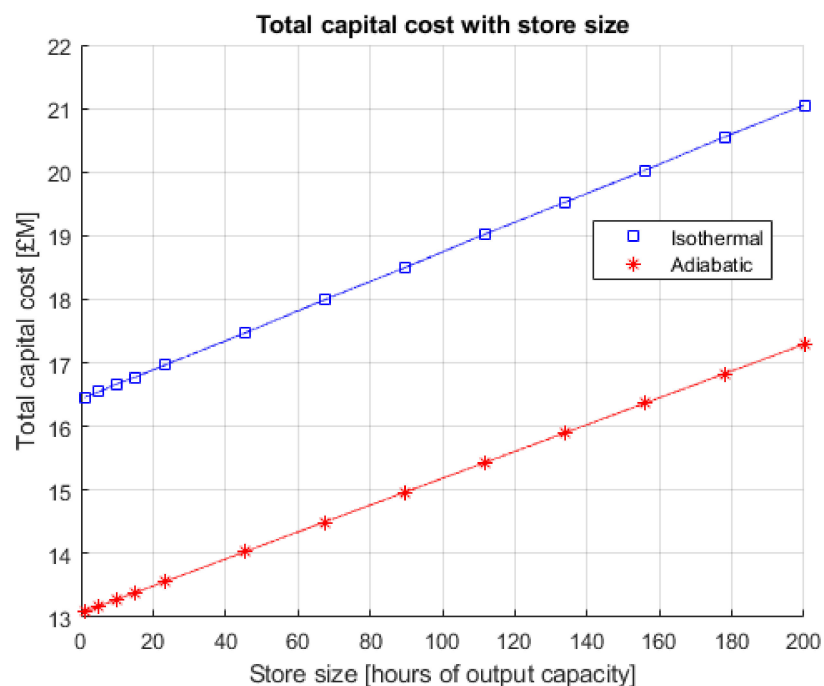


Figure 16. The relationship between total system cost and storage capacity for a representative system with the maximum allowable inlet swept volume.

For the isothermal case, the maximum ROI at each site ranged from 6.4% to 9.8%. For the adiabatic case, the maximum ROI ranged from 8.1% to 13.0%. At all sites, this maximum occurred at the highest value of swept volume, with the optimal store size varying only slightly.

The lowest ROI values (between 0.8% and 1% for the isothermal case and between 1.8% and 2.4% for the adiabatic case) are found when the swept volume is at its lowest and the storage capacity is close to zero, due to the high system costs and minimal benefit provided by the store.

In the adiabatic case, at higher values of swept volume, the air reaches temperatures nearing the limits of sensible heat storage capabilities (~900 K). This could be accounted for with multi-stage adiabatic compression utilising inter-stage cooling.

Using the method and values described in this paper, it seems likely that an adiabatic wind-driven compressor is significantly financially favourable over an isothermal one for the *Wi-DACIS* system. It is advantageous to design the system such that the wind-driven compressor performs the majority of the total work, achieved by designing for maximum swept volume and adiabatic operation. The existence of an optimal store size in each case is also of interest, as it creates a clear system design goal for store size—something that is not seen to be the case for standalone storage in Section 4.5.

4.4. Validation

In addition to the real wind and electricity price data used in this paper, and the nominal costs and efficiencies based on prior literature, data validation was performed in the form of a Monte Carlo simulation. The ranges of cost and efficiency shown in Tables 3 and 4 were used to create triangular probability distributions for each parameter. For each iteration of the *Wi-DACIS* system (characterised by the values of V_{swept} and store size), random weighted samplings of these distributions were created, and the cost, income, expenditure, profit and ROI values of that iteration were adjusted accordingly. With 10^5 runs in each iteration, a normal distribution was then fit to the result, and the coefficient of variation (that is, the standard deviation normalised by the mean and presented as a percentage) of the ROI was found, as shown in Figure 17.

The coefficient of variation is considerably higher at low values of V_{swept} . At its highest, it reaches 141% in the isothermal case and 51% in the adiabatic case. This is due to the low mean ROI values and higher proportional power of COMG at the minimum swept volume. For some values of cost and efficiency, the ROI at these low V_{swept} iterations can be negative, a result of the losses in the system outweighing the benefits of absorbing and storing the electricity. Clearly a system with such parameters would not be economically viable.

However, at middling and higher values of V_{swept} , the coefficient of variation quickly becomes tolerable, plateauing at around 10–15% for the isothermal case and 7–10% for the adiabatic case. As with the effects of V_{swept} on the variability, the isothermal case is more variable due to the larger proportional power of COMG, resulting in lower profit margins and more chance for an expensive compressor to impact the ROI of the system.

Given that the iterations that have been shown to be more favourable are those with higher values of V_{swept} , the variability calculated due to possible variations in the input parameters is considered to be acceptable.

4.5. Comparison with Other Systems

Comparing the ROI and capital costs of the *Wi-DACIS* system with alternative wind-storage options is useful in determining whether the system described here has a potential place in the energy grid.

A conventional 8 MW wind turbine (capital cost ~£8 M) on the CfD scheme with a strike price of 40 GBP/MWh has a maximum ROI of 22% using the same wind and price data. Approximately the same maximum ROI was found for a free-market wind turbine over the same time period. The difference in the ROI between these turbines and the

Wi-DACIS system supports the generally held belief that it is much more expensive to store a unit of energy than it is to generate it.

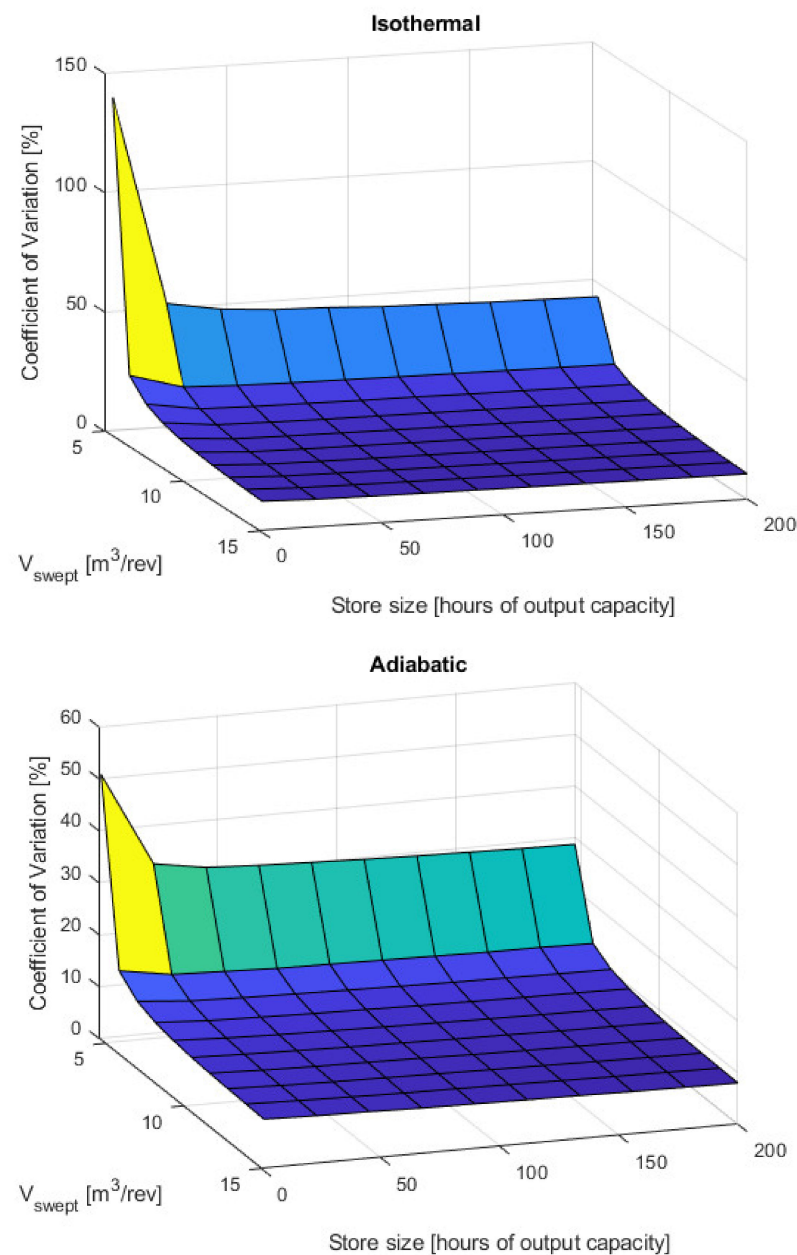


Figure 17. Results of data validation for isothermal (**above**) and adiabatic (**below**) systems, presented as the coefficient of variation of the ROI for each iteration.

However, given the necessity for large-scale storage in future energy grids, regardless of its relative profitability, it is useful to compare like-for-like. Therefore, two other wind-storage systems have been simulated, using the same initial logic: a wind turbine with co-located Li-ion battery storage, and a wind turbine connected to both a compressed air energy store (CAES) and the grid.

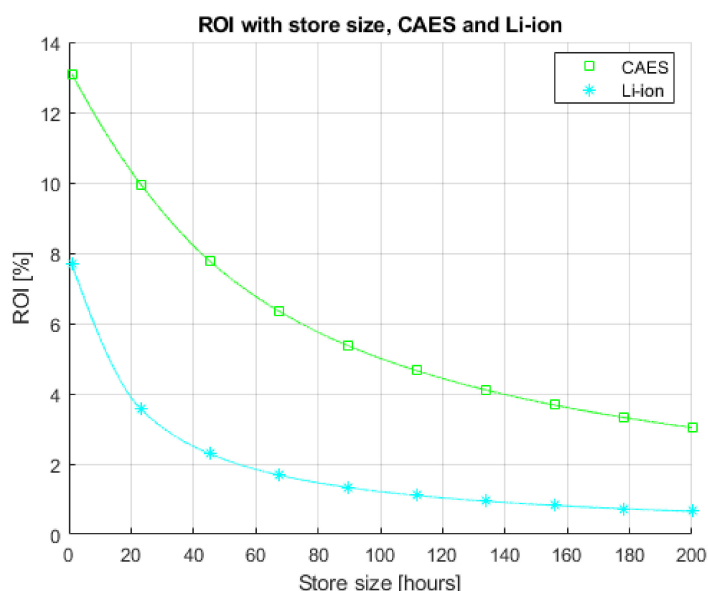
The efficiencies and costs assumed for these systems are summarised in Table 5.

Table 5. Efficiencies and costs of the other wind–storage systems. Costs estimated from [49,50].

Name of Parameter	Li-Ion Store	CAES Store	Units
Efficiency	0.9	0.65	-
Cost (capacity)	150	20	£/kWh
Scale (capacity)	8–1600	8–1600	MWh
Cost (power)	1500	300	£/kW

The efficiencies were applied in a similar approach as the *Wi-DACIS* simulation. During costing, the store was considered larger by a factor $\sqrt{\eta}$ (to apply the same efficiency loss to the beginning and the end of the process), and during revenue calculations, income was reduced by the same factor.

The wind turbine was considered to be acting on the free market in both cases, and the same algorithm (based on [36]) was used to decide whether to sell or store energy, where possible. The power costs provided in Table 5 are the total costs for charging and discharging power. As with the *Wi-DACIS* system, the storage capacity was calculated in hours, from 1 to 200. Figure 18 shows the representative ROI curves for the two systems.

**Figure 18.** The relationship between one-year return on investment and storage capacity for the Li-ion and CAES simulations.

For a set storage capacity, the Li-ion system achieves higher revenue in all cases (due, obviously, to the only simulated difference in the income of the two systems being their efficiencies). However, the CAES system achieves significantly higher ROI values. The maximum ROI values for CAES were between 9.7% and 14.3% and were between 4.9% and 8.4% for Li-ion. These all occur during the lowest possible store size. Comparing Figures 14 and 18, it appears as though the *Wi-DACIS* system is extremely competitive with alternative storage systems, especially at higher storage capacities. Section 4.6 discusses an interesting quirk of *Wi-DACIS* that may give it further viability, from a whole grid perspective.

4.6. Capture Value

The capture value (CV) of a wind turbine is a measure of how effectively the turbine can achieve the average electricity value over a given time period. Wind power generally has a negative correlation with electricity price—during times of high wind, the wind

fleet of a grid is generating more electricity, increasing supply, and thereby reducing the electricity price. Capture value is calculated as:

$$CV = \frac{\sum_{i=1}^n output_i \times price_i}{price \times \sum_{i=1}^n output_i}, \quad (18)$$

where *output* and *price* are the wind electricity output and electricity price at time *i*, and \overline{price} is the average electricity price over the time period [51].

The average capture values are expected to decrease in the future, due to significantly increased wind generation capacity. This is a concern for wind farm operators, due to the uncertainty it creates [51,52]. Less certainty in wind farm output may result in reduced investment in wind farms in the future.

Any system that stores exergy prior to sending electricity to the grid has the potential to lessen the negative impact of this capture value, both for itself (by only selling during times of high electricity price) and for the whole grid (by reducing the wind supply during times of high wind). *Wi-DACIS* is an example of such a system, but so is any co-located wind-storage system. What sets *Wi-DACIS* apart is that it also draws electricity from the grid when the wind turbine is working, via its grid-powered compressor. Because the instantaneous power of this compressor is directly proportional to the instantaneous wind resource, *Wi-DACIS* would serve to draw electricity mainly at times of high wind. When this coincides with times of low electricity value (which will occur increasingly more frequently), *Wi-DACIS* will store this energy. Through this mechanism, *Wi-DACIS* further lessens the capture value problem. This improved capture value could reduce uncertainty in future wind farm investments. However, any system intending to make a significant impact on the capture value of a whole grid would need to account for a significant proportion of the wind generation capacity of that grid.

5. Summary

The wind-driven GIES system described in this paper has the potential to offer significant generation flexibility to wind power generation. Further costing work must be done before the economic case is fully made. By including some electrically driven compression prior to supplying air to the wind-driven compressor, a solution is found to the problem that large intake swept volumes would otherwise be needed. This allows direct drive machinery to replace the expensive gearbox system in a conventional turbine.

The use of underwater compressed air energy storage in the form of flexible energy bags has natural synergy with floating offshore wind turbines, which may be situated over extremely deep water. It has been shown in a previous paper that these energy bags have an optimum diameter, which was suggested to be approximately 20 m. Any energy store utilising these bags should therefore employ multiple optimally sized bags.

For multiple configurations of the system, simulations were run for both an adiabatic and an isothermal wind-driven compressor. For a set wind turbine and upper pressure, as the allowable volumetric swept intake of the main stage compressor increases:

- The pressure ratio of the grid-powered compressor reduces and the pressure ratio of the wind-driven compressor increases;
- The power ratio between the wind-driven and grid-powered compressors increases; and
- The one-year return on investment of the system increases.

It is therefore desirable to accommodate the maximum possible swept volume.

It was also found that the adiabatic main stage compressor achieved higher ROI values than the isothermal configuration. This is partly due to the relatively cheap thermal energy storage used in the adiabatic case. The adiabatic case also results in a more favourable ratio of wind-driven to grid-powered compressor powers, resulting in a configuration closer to a pure generation-integrated energy storage system.

There is an optimum value of store size for ROI with the *Wi-DACIS* system, which is generally between 10 and 20 h of rated output. With proper design and sizing, ROI values

in the region of 10–15% are certainly possible. A Monte Carlo simulation validated the assumed costs of the system by showing low variability (in the order of 10%) at higher values of V_{swept} , where these ROI values were found.

With the wind data used in this paper, a conventional wind turbine achieves higher ROI values than the *Wi-DACIS* system. However, under the same assumptions, the other wind–storage systems simulated also achieved lower ROI values than the conventional turbine, and the optimum values for these systems were found at the minimum storage capacity, which most closely resembles a standalone wind turbine. The *Wi-DACIS* system performed as well as or better than the alternative storage solutions, especially at higher storage capacities.

The addition of a medium-pressure store may serve to add flexibility to the system, reducing the expenditure by allowing *Wi-DACIS* to draw energy from the grid at times of lower electricity value. This additional store should be analysed in future work.

Further analysis should also be performed on the relative costs of the system elements, as these will dictate proper sizing. The effect that the power ratio between the two compressors has on the overall efficiency of the system is of interest, as an iteration that is closer to standalone storage than GIES may result in a less efficient system. The benefit of overrating of the expander, allowing for quicker discharge of the high-pressure store, should also be investigated.

In this paper, the efficiency of the wind-driven compressor was given in relative terms, with the assumption being that it would be as efficient as a traditional wind turbine transmission system. This should be verified as the development of the adiabatic compressor in [6] continues.

With a sufficient grid presence, *Wi-DACIS* may also act as a capture value balancer, due to its dual mechanisms of storing energy during times of low electricity price (which will increasingly frequently occur during times of high wind) and drawing electricity from the grid during times of high wind availability, thereby increasing demand. With a significant market share of the wind generation capacity of a grid, *Wi-DACIS* could greatly reduce the uncertainty surrounding capture value in wind farms. Further work should be done to determine the value of the *Wi-DACIS* and similar wind-driven systems in an expected future energy network, as the negative correlation between electricity price and wind availability becomes more pronounced in the coming years. This negative correlation may heavily impact conventional wind farms that lack co-located energy storage, at which point systems such as *Wi-DACIS* may have an extremely promising economic case.

Author Contributions: Conceptualization, L.S.-S., S.D.G. and D.G.; methodology, L.S.-S. and S.D.G.; software, L.S.-S. and B.C.; validation, L.S.-S. and B.C.; formal analysis, L.S.-S.; investigation, L.S.-S.; writing—original draft preparation, L.S.-S.; writing—review and editing, L.S.-S., S.D.G., D.G. and J.P.R.; visualization, L.S.-S.; supervision, S.D.G., D.G. and J.P.R.; project administration, S.D.G.; funding acquisition, S.D.G. All authors have read and agreed to the published version of the manuscript.

Funding: The authors would like to thank the United Kingdom’s Engineering and Physical Sciences Research Council (EPSRC) for funding this work through the following research grants: ‘Multi-scale Analysis for Facilities for Energy Storage’ (Manifest: EP/N032888/1) and ‘Generation Integrated Energy Storage - A Paradigm Shift’ (EP/P023320/1).

Data Availability Statement: Restrictions apply to the availability of wind speed data. Data was obtained from NCAS British Atmospheric Data Centre and the post-processed data are available from the authors with permission of NCAS British Atmospheric Data Centre. Publicly available day-ahead electricity price data were analysed in this study. This data can be found here: <https://transparency.entsoe.eu/dashboard/show>. The outcome data presented in this study are available upon reasonable request from the corresponding author.

Conflicts of Interest: The authors declare no conflict of interest.

Nomenclature

<i>C</i>	cost [GBP]
<i>D</i>	diameter [m]
<i>E</i>	energy [J]
<i>f</i>	frequency [1/s]
<i>F</i>	force [N]
<i>L</i>	length [m]
<i>m</i>	mass [kg]
<i>p</i>	pressure [bar]
<i>P</i>	power [W]
<i>r</i>	ratio of pressures
<i>T</i>	temperature [K]
<i>u</i>	(wind) speed [m/s]
<i>V</i>	volume [m ³]
<i>W</i>	work [J]
<i>z</i>	altitude [m]
γ	ratio of specific heats
η	efficiency
κ	Von Kármán constant
ω	rotational speed [rad/s]

Subscripts and Superscripts

<i>0</i>	roughness length
<i>1</i>	inlet stage 1 (pressure, volume)
<i>2</i>	outlet stage 1/inlet stage 2 (pressure, volume)
<i>3</i>	outlet stage 2 (pressure, volume)
<i>ADIA</i>	adiabatic
<i>G</i>	grid (pressure ratio)
<i>Heat</i>	heat (energy)
<i>ISO</i>	isothermal
<i>opt</i>	optimal (volume)
<i>quartz</i>	quartz (mass)
<i>ref</i>	reference (temperature)
<i>steel</i>	steel (mass)
<i>store</i>	thermal store (temperature, volume)
<i>swept</i>	swept (volume) per rev
<i>T</i>	tension (force)
<i>TIP</i>	wind turbine blade tip (speed)
<i>turbine</i>	turbine (power)
<i>W</i>	wind (pressure ratio)
<i>*</i>	friction velocity

Abbreviations

<i>AB</i>	anchoring ballast
<i>A-CAES</i>	adiabatic compressed air energy storage
<i>CAES</i>	compressed air energy storage
<i>CfD</i>	contracts for difference
<i>COMG</i>	compressor (grid-driven)
<i>COMW</i>	compressor (wind-driven)
<i>CV</i>	capture value
<i>D-CAES</i>	diabatic compressed air energy storage
<i>EXP</i>	expander
<i>GIES</i>	generation-integrated energy storage
<i>HPEB</i>	high-pressure energy bag
<i>HXU</i>	heat exchanger unit
<i>I-CAES</i>	isothermal compressed air energy storage

MIDAS	Met Office Integrated Data Archive System
ROI	return on investment
SoC	state of charge
SU	canvas surface
TC	tension cables
TES	thermal energy storage
TSR	tip-speed ratio
UWCAES	underwater compressed air energy storage
Wi-DACIS	wind-driven air compression and isobaric storage

References

1. Cárdenas, B.; Swinfen-Styles, L.; Rouse, J.; Garvey, S.D. Short-, Medium-, and Long-Duration Energy Storage in a 100% Renewable Electricity Grid: A UK Case Study. *Energies* **2021**, *14*, 8524. [CrossRef]
2. Garvey, S.D.; Eames, P.C.; Wang, J.H.; Pimm, A.J.; Waterson, M.; MacKay, R.S.; Giulietti, M.; Flatley, L.C.; Thomson, M.; Barton, J.; et al. On Generation-Integrated Energy Storage. *Energy Policy* **2015**, *86*, 544–551. [CrossRef]
3. Dunn, R. A global review of concentrated solar power storage. In Proceedings of the Solar2010, the 48th AuSES Annual Conference, 1–3 December 2010; p. 10.
4. Bergan, P.G.; Greiner, C.J. A New Type of Large Scale Thermal Energy Storage. *Energy Proc.* **2014**, *58*, 152–159. [CrossRef]
5. Ingersoll, E.; Marcus, D.R. Wind Turbine System. U.S. Patent Application 11/804,704, 28 February 2008.
6. Garvey, S.D.; Pimm, A.J.; Buck, J.A.; Woolhead, S.; Liew, K.W.; Kantharaj, B.; Garvey, J.E.; Brewster, B.D. Analysis of a Wind Turbine Power Transmission System with Intrinsic Energy Storage Capability. *Wind. Eng.* **2015**, *39*, 149–173. [CrossRef]
7. Salter, S.H.; Rea, M. Hydraulics for Wind. In Proceedings of the European Wind Energy Conference, Hamburg, Germany, 22–26 October 198; pp. 534–541.
8. Lee, J.L. On-Demand Generation of Electricity from Stored Wind Energy. U.S. Patent 8,664,793, 4 March 2014.
9. Ren, Z.; Wang, H.; Chen, G.; Li, X.; Esfarjani, K. Metallic Composite Phase-Change Materials and Methods of Using the Same. U.S. Patent US2014109895A1, 24 April 2014.
10. Denholm, P.; King, J.C.; Kutcher, C.F.; Wilson, P.P.H. Decarbonizing the Electric Sector: Combining Renewable and Nuclear Energy Using Thermal Storage. *Energy Policy* **2012**, *44*, 301–311. [CrossRef]
11. Swinfen-Styles, L.; Garvey, S.D.; Giddings, D. Combining Wind-Driven Air Compression with Underwater Compressed Air Energy Storage. In Proceedings of the Offshore Energy and Storage Summit (OSES), Brest, France, 10–12 July 2019. [CrossRef]
12. Wang, J.; Lu, K.; Ma, L.; Wang, J.; Dooner, M.; Miao, S.; Li, J.; Wang, D. Overview of Compressed Air Energy Storage and Technology Development. *Energies* **2017**, *10*, 991. [CrossRef]
13. Rogers, A.; Henderson, A.; Wang, X.; Negnevitsky, M. Compressed Air Energy Storage: Thermodynamic and Economic Review. In Proceedings of the IEEE PES General Meeting | Conference & Exposition, National Harbor, MD, USA, 27–31 July 2014. [CrossRef]
14. Safaei, H.; Aziz, M.J. Thermodynamic Analysis of Three Compressed Air Energy Storage Systems: Conventional, Adiabatic, and Hydrogen-Fueled. *Energies* **2017**, *10*, 1020. [CrossRef]
15. Dufo-López, R.; Bernal-Agustín, J.L.; Domínguez-Navarro, J.A. Generation Management Using Batteries in Wind Farms: Economical and Technical Analysis for Spain. *Energy Policy* **2009**, *37*, 126–139. [CrossRef]
16. Cavallo, A. Controllable and Affordable Utility-Scale Electricity from Intermittent Wind Resources and Compressed Air Energy Storage (CAES). *Energy* **2007**, *32*, 120–127. [CrossRef]
17. Bennett, J.A.; Simpson, J.G.; Qin, C.; Fittro, R.; Koenig, G.M.; Clarens, A.F.; Loth, E. Techno-Economic Analysis of Offshore Isothermal Compressed Air Energy Storage in Saline Aquifers Co-Located with Wind Power. *Appl. Energy* **2021**, *303*, 117587. [CrossRef]
18. Matsuo, T.; Okazaki, T. A Basic Theory of Induction Heating for a Wind-Powered Thermal Energy System. *IEEE Trans. Magn.* **2017**, *53*, 1–5. [CrossRef]
19. Li, P.Y.; Loth, E.; Simon, T.W.; Van de Ven, J.D.; Crane, S.E. Compressed air energy storage for offshore wind turbines. In Proceedings of the International Fluid Power Exhibition (IFPE), Las Vegas, NV, USA, 23–25 March 2011.
20. Ribrant, J.; Bertling, L. Survey of Failures in Wind Power Systems with Focus on Swedish Wind Power Plants during 1997–2005. In Proceedings of the IEEE Power Engineering Society General Meeting, Tampa, FL, USA, 24–28 June 2007. [CrossRef]
21. Ragheb, A.; Ragheb, M. Wind Turbine Gearbox Technologies. In Proceedings of the 1st International Nuclear & Renewable Energy Conference (INREC), Amman, Jordan, 21–24 March 2010. [CrossRef]
22. Daneshi-Far, Z.; Capolino, G.A.; Henao, H. Review of Failures and Condition Monitoring in Wind Turbine Generators. In Proceedings of the XIX International Conference on Electrical Machines—ICEM, Rome, Italy, 6–8 September 2010. [CrossRef]
23. Bauer, L.; Matysik, S. Wind-Turbine-Models. Available online: <https://en.wind-turbine-models.com/turbines/1419-mhi-vestas-offshore-v164-8.0-mw> (accessed on 10 February 2022).
24. Smallbone, A.; Jülch, V.; Wardle, R.; Roskilly, A.P. Levelised Cost of Storage for Pumped Heat Energy Storage in Comparison with Other Energy Storage Technologies. *Energy Convers. Manag.* **2017**, *152*, 221–228. [CrossRef]
25. Kim, Y.M.; Shin, D.G.; Favrat, D. Operating Characteristics of Constant-Pressure Compressed Air Energy Storage (CAES) System Combined with Pumped Hydro Storage Based on Energy and Exergy Analysis. *Energy* **2011**, *36*, 6220–6233. [CrossRef]

26. Pimm, A.J.; Garvey, S.D.; Drew, R.J. Shape and Cost Analysis of Pressurized Fabric Structures for Subsea Compressed Air Energy Storage. *Proc. Inst. Mech. Eng. Part C J. Mech. Eng. Sci.* **2011**, *225*, 1027–1043. [CrossRef]
27. Pimm, A.J.; Garvey, S.D.; de Jong, M. Design and Testing of Energy Bags for Underwater Compressed Air Energy Storage. *Energy* **2014**, *66*, 496–508. [CrossRef]
28. Moradi, J.; Shahinzadeh, H.; Khandan, A.; Moazzami, M. A Profitability Investigation into the Collaborative Operation of Wind and Underwater Compressed Air Energy Storage Units in the Spot Market. *Energy* **2017**, *141*, 1779–1794. [CrossRef]
29. Astolfi, M.; Guandalini, G.; Belloli, M.; Hirn, A.; Silva, P.; Campanari, S. Preliminary Design and Performance Assessment of an Underwater CAES System (UW-CAES) for Wind Power Balancing. In Proceedings of the Volume 3: Coal, Biomass, Hydrogen, and Alternative Fuels; Cycle Innovations; Electric Power; Industrial and Cogeneration, Organic Rankine Cycle Power Systems, Phoenix, AZ, USA, 17–21 June 2019. [CrossRef]
30. Met Office (2012): Met Office Integrated Data Archive System (MIDAS) Land and Marine Surface Stations Data (1853–Current; 2015 Used); NCAS British Atmospheric Data Centre. Available online: <https://catalogue.ceda.ac.uk/uuid/dbd451271eb04662beade68da43546e1> (accessed on 20 March 2018).
31. Holmes, J.D.; Paton, C.; Kerwin, R. *Wind Loading of Structures*; CRC Press: Boca Raton, FL, USA, 2007. [CrossRef]
32. Wieringa, J. Updating the Davenport Roughness Classification. *J. Wind. Eng. Ind. Aerodyn.* **1992**, *41*, 357–368. [CrossRef]
33. Google. Google Maps. Available online: <https://www.google.com/maps> (accessed on 20 March 2018).
34. Databayou. World Ocean Depth Map. 2021. Available online: <https://databayou.com/ocean/depth.html> (accessed on 25 November 2021).
35. ENTSO-E Transparency Platform. UK Day-Ahead Electricity Prices. Online Dataset. Available online: <https://transparency.entsoe.eu/dashboard/show> (accessed on 20 June 2020).
36. Connolly, D.; Lund, H.; Finn, P.; Mathiesen, B.V.; Leahy, M. Practical Operation Strategies for Pumped Hydroelectric Energy Storage (PHES) Utilising Electricity Price Arbitrage. *Energy Policy* **2011**, *39*, 4189–4196. [CrossRef]
37. Pelay, U.; Luo, L.; Fan, Y.; Stitou, D.; Rood, M. Thermal Energy Storage Systems for Concentrated Solar Power Plants. *Renew. Sustain. Energy Rev.* **2017**, *79*, 82–100. [CrossRef]
38. Safaei, H.; Keith, D.W.; Hugo, R.J. Compressed Air Energy Storage (CAES) with Compressors Distributed at Heat Loads to Enable Waste Heat Utilization. *Appl. Energy* **2013**, *103*, 165–179. [CrossRef]
39. Arsalis, A. Thermo-economic Modeling and Parametric Study of Hybrid SOFC–Gas Turbine–Steam Turbine Power Plants Ranging from 1.5 to 10MWe. *J. Power Sources* **2008**, *181*, 313–326. [CrossRef]
40. Akrami, E.; Chitsaz, A.; Nami, H.; Mahmoudi, S.M.S. Energetic and Exergoeconomic Assessment of a Multi-Generation Energy System Based on Indirect Use of Geothermal Energy. *Energy* **2017**, *124*, 625–639. [CrossRef]
41. Luyben, W.L. Capital Cost of Compressors for Conceptual Design. *Chem. Eng. Processing Process Intensif.* **2018**, *126*, 206–209. [CrossRef]
42. Mashimo, T.; Ariga, I.; Sakai, T.; Watanabe, I. On the Performance Prediction of a Centrifugal Compressor Scaled Up. In Proceedings of the Volume 1: Turbomachinery, London, UK, 18–22 April 1982. [CrossRef]
43. Chen, H. Size and Reynolds Number Effects on Compressor Performance and Scaling. In Proceedings of the Volume 2E: Turbomachinery, Virtual, Online, 21–25 September 2020. [CrossRef]
44. Ebadollahi, M.; Rostamzadeh, H.; Ghaebi, H.; Amidpour, M. Exergoeconomic Analysis and Optimization of Innovative Cascade Bi-Evaporator Electricity/Cooling Cycles with Two Adjustable Cooling Temperatures. *Appl. Therm. Eng.* **2019**, *152*, 890–906. [CrossRef]
45. Aali, A.; Pourmahmoud, N.; Zare, V. Exergoeconomic Analysis and Multi-Objective Optimization of a Novel Combined Flash-Binary Cycle for Sabalan Geothermal Power Plant in Iran. *Energy Convers. Manag.* **2017**, *143*, 377–390. [CrossRef]
46. Weiner, D.; Shnaid, I. Second-Law Analysis of a Compressed Air Energy Storage (CAES) System. In Proceedings of the Volume 4: Heat Transfer; Electric Power; Industrial and Cogeneration, Cologne, Germany, 1–4 June 1992. [CrossRef]
47. Courtois, N.; Najafiyazdi, M.; Lotfalian, R.; Boudreault, R.; Picard, M. Analytical Expression for the Evaluation of Multi-Stage Adiabatic-Compressed Air Energy Storage (A-CAES) Systems Cycle Efficiency. *Appl. Energy* **2021**, *288*, 116592. [CrossRef]
48. Houssainy, S.; Janbozorgi, M.; Kavehpour, P. Thermodynamic Performance and Cost Optimization of a Novel Hybrid Thermal-Compressed Air Energy Storage System Design. *J. Energy Storage* **2018**, *18*, 206–217. [CrossRef]
49. Steward, D.; Saur, G.; Penev, M.; Ramsden, T. *Lifecycle Cost Analysis of Hydrogen Versus Other Technologies for Electrical Energy Storage*; Technical Report; NREL: Golden, CO, USA, 2009.
50. Argyrou, M.C.; Christodoulides, P.; Kalogirou, S.A. Energy Storage for Electricity Generation and Related Processes: Technologies Appraisal and Grid Scale Applications. *Renew. Sustain. Energy Rev.* **2018**, *94*, 804–821. [CrossRef]
51. Jansen, M.; Staffell, I.; Kitzing, L.; Quoilin, S.; Wiggelinkhuizen, E.; Bulder, B.; Riepin, I.; Müsgens, F. Offshore Wind Competitiveness in Mature Markets without Subsidy. *Nat. Energy* **2020**, *5*, 614–622. [CrossRef]
52. Impacts of Inter-Annual Wind and Solar Variations on the European Power System. *Joule* **2018**, *2*, 2076–2090. [CrossRef]